nature communications

Article

https://doi.org/10.1038/s41467-024-53043-5

Vitrimer-like elastomers with rapid stress-relaxation by high-speed carboxy exchange through conjugate substitution reaction

Received: 25 March 2024

Accepted: 27 September 2024

Published online: 05 October 2024

Check for updates

Natsumi Nishiie[1], Ryo Kawatani[1], Sae Tezuka[1], Miu Mizuma[1], Mikihiro Hayashi[2] ✉ & Yasuhiro Kohsaka[1,3] ✉

We report vitrimer-like elastomers that exhibit significantly fast stress relaxation using carboxy exchange via the conjugate substitution reaction of α-(acyloxymethyl) acrylate skeletons. This network design is inspired by a small-molecule model that shows the carboxy exchange reaction even at ambient temperature in the presence of 1,4-diazabicyclo[2.2.2]octane (DABCO). The acrylate and acrylic acid copolymers are cross-linked using bis[α-(bromomethyl)acrylates] and doped with 10 wt% DABCO, exhibiting processability to obtain a transparent film by hot pressing. The high-speed bond exchange in the network, validated by stress-relaxation tests, allows quick molding with household iron. In addition, the material is applied as an adhesion sheet for plastic and metal substrates. Because dynamic cross-linking with the proposed bond exchange mechanism can be implemented for any polymer bearing carboxyl pendants, our approach can be applied to versatile backbones, which must thus be meaningful in the practical sense.

Vitrimers are a new class of cross-linked polymers proposed by Leibler et al.[1], and are defined as network polymers cross-linked by dynamic covalent bonds (DCBs) that can undergo thermal or photo-activated associative bond exchange[1]. Bond exchange in the network realizes useful functions, including recyclability, healability, reprocessability, and weldability[2,3]. The meaning of associative bond exchange in vitrimers is occurrence of the new bond formation before the dissociation of original bond pair, through the associated intermediates, such as in the cases of addition–elimination and metathesis mechanisms[4,5]. Owing to the associative bond-exchange mechanism, the cross-linking points of the vitrimer networks are always preserved during bond exchange. Therefore, vitrimers exhibit unique rheological and flow properties, such as Arrhenius dependence of viscosity or relaxation time in the molten state[6,7], which is completely different from conventional polymer materials such as thermoplastics and thermosets. Notably, there is different, but similar type of materials, called vitrimer-like materials. Such materials exhibit the feature of the Arrhenius dependency, although the bond exchange passes through dissociative bond exchange mechanism. In this case, the dissociated state is immediately converted back to the associated state due to the energetic favorability, during which the bond pair is exchanged. To distinguish them from true vitrimers, these materials are termed as vitrimer-like materials[8–10].

Transesterification catalyzed by Lewis acids or bases is among the most typical bond exchange reactions used for vitrimers because the bond exchange is sufficiently slow to be ignored at room temperature, but fast enough to induce processability at elevated temperatures[11]. For a similar reason, the bond-exchange of vinylogous urethane and boronic ester have been applied to vitrimers[12]. Notably, the relaxation dynamics is one of the key factors governing the performances of vitrimers[13]. For example, recent research has demonstrated a correlation between healability/recyclability and relaxation rate. Although various molecular parameters, such as the cross-link density and fraction of bond exchangeable units, are known to influence the

[1]Faculty of Textile Science and Technology, Shinshu University, 3-15-1 Tokida, Ueda, Nagano 386-8567, Japan. [2]Department of Life Science and Applied Chemistry, Graduate School of Engineering, Nagoya Institute of Technology, Gokiso-cho Showa-ku, Nagoya, Aichi 466-8555, Japan. [3]Research Initiative for Supra-Materials (RISM), Interdisciplinary Cluster for Cutting Edge Research (ICCER), Shinshu University, 4-17-1 Wakasato, Nagano 380-8553, Japan. ✉e-mail: hayashi.mikihiro@nitech.ac.jp; kohsaka@shinshu-u.ac.jp

relaxation properties, the relaxation rate is essentially governed by the kinetics of the bond exchange reaction as the primary process. Therefore, the introduction of fast bond exchange reactions into vitrimers or vitrimer-like materials is expected to achieve the efficient generation of functions, although the types of such reactions are not sufficiently explored.

Recently, allyl-substituted Michael acceptors (Fig. 1A) has gained attention as a toolbox for chemical reaction networks (CRN)[14,15]. For example, Eelkema and coworkers have reported CRN using conjugate addition–substation reactions of α-(acetoxymethyl)vinylphosphonate as a reversible state change of polymers between micellar assembly and hydrogels[16]. On the other hand, we have reported the application of the thiol exchange reaction of α-(thiomethyl)acrylate for cross-linking and de-crosslinking at ambient temperature[17]. In thiol-exchange reaction, the equilibrium includes the both the substitution products (State I and III) and the addition product (State II). In contrast, some studies have implied a fast reversible carboxy-exchange reaction that does not afford an addition product (Fig. 1B)[18–20]; this type of reaction is called conjugate substitution[21,22]. In this study, we provide a detailed investigation of the carboxy-exchange reaction by assessing the availability of a promising candidate for bond exchange mechanism driven at a fast rate. Then, the carboxy-exchange reaction was incorporated into relatively simple polyacrylate networks; although the carboxy-exchange reaction should pass through dissociative bond exchange, the material exhibited Arrhenius dependence of relaxation time over a broad temperature range, and thus can be admitted as a vitrimer-like material. Owing to the high-rate bond exchange, significantly fast relaxation is achieved, leading to a new design of vitrimer-like materials that can exhibit useful functions under mild and quick processes.

Results and discussion

Model carboxy-exchange reaction by conjugate substitution reaction

To examine the potential for carboxy-exchange by the conjugate substitution reaction, methyl α-(acetoxymethyl)acrylate (**1a**) was treated with benzoic acid (**2b**) in deuterated chloroform ($CDCl_3$) in the presence of 1,4-diazabicyclo[2.2.2]octane (DABCO) (Fig. 1B). The ^{1}H NMR spectrum of the reaction mixture after 36 h showed a new set of signals (Figs. 1C, 6.4 and 5.9 ppm for vinylidene protons, and 4.9 ppm for allylic protons), suggesting the generation of α-(benzoyloxymethyl)acrylate (**1b**). Figure 1D shows the change of molar fraction of **1a** estimated as an intensity ratio of allylic-proton signals (4.7 ppm for **1a** and 4.9 ppm for **1b**, respectively). The reaction system reached equilibrium within 9 h at 25 °C, which suggested a reversible carboxy-exchange reaction. Notably, no reactions were observed using

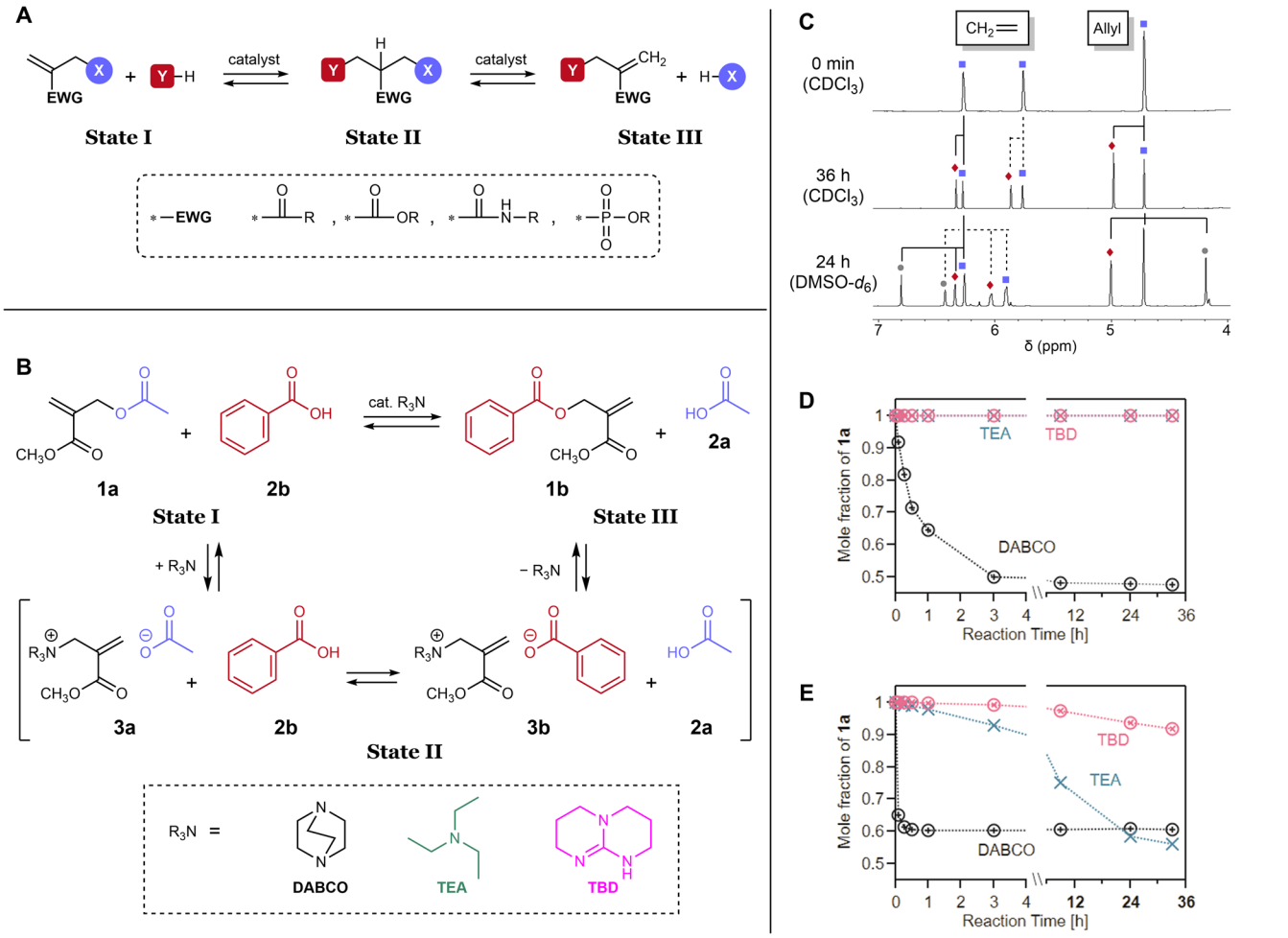

Fig. 1 | Model reaction of carboxy-exchange by conjugate substitution. A Allyl-substituted Michael acceptors for CRN. **B** Model carboxy-exchange by conjugate substitution reaction. **C** ^{1}H NMR spectral changes before and after carboxy exchange using DABCO catalyst (400 MHz, 25 °C, solvents for each spectrum are shown in legends). The labels for the signal assignments are corresponding to those in **B**. The gray circles are assignable to both **3a** and **3b**. The full-scale spectra are shown in Fig. S1 and Fig. S4D, E: Changes in the molar fraction of **1a** during the carboxy-exchange in $CDCl_3$ (**D**) and DMSO (**E**) in the presence of various amine catalysts. The raw data from the ^{1}H NMR spectra are shown in Figs. S1–S7.

triethylamine (TEA) and 1,5,7-triazabicyclo[4.4.0]dec-5-ene (TBD) as the catalysts with lower nucleophilicity than DABCO. These results suggest that the formation of ammonium intermediates (**3a** and **3b**) is the key to promoting the reaction because the nucleophilicity of the tertiary amine catalyst significantly affects the reaction rate.

A similar reaction was performed using DABCO in deuterated dimethyl sulfoxide (DMSO-d_6) at 25 °C. The ^{1}H NMR spectra (Fig. 1C) of the reaction mixture after 24 h shows a set of signals (6.8, 6.4 ppm for vinylidene protons and 4.2 ppm for allylic proton) different from **1a** and **1b**. This suggested the existence of ammonium intermediates **3a** and **3b**, stabilized by the solvation of DMSO. The detailed characterization is presented in Supplementary Information (section 2, Fig. S5, Table S1). The decrease in **1a** (Fig. 1E) indicated that the reaction system almost reached equilibrium after 5 min, and was completed after 30 min. TEA and TBD also functioned as catalysts in DMSO, although their reaction rates were lower than that in the presence of DABCO. Therefore, the polar environment was effective in stabilizing ammonium intermediates and promoting carboxy exchange. The ammonium intermediate was observed in a co-solvent of DMSO-d_6 and $CDCl_3$ (v/v = 1/1, Fig. S8) as a set of weak ^{1}H NMR signals, implying that a significant amount of donor solvent was required to stabilize the ammonium intermediate.

Preparation of cross-linked polymers

The above model reactions revealed that the carboxy exchange by conjugate substitution reaction progressed even at 25 °C, the rate of which was dependent on solvent polarity. Because the polarity and diffusivity of the molecules are significantly different between the solution and bulk systems, the results of the model reactions do not immediately indicate their applicability to vitrimer-like elastomers. Nonetheless, the fast bond exchange in the model reaction led us to expect the development of new type of vitrimer-like materials with fast relaxation dynamics. Note that the carboxy exchange is classified as 'dissociative' bond-exchange because it goes through a non-covalent ammonium intermediate as described in the previous section, so the target of this research should be regarded as vitrimer-like elastomers rather than true vitrimers. Radical copolymerization of ethyl acrylate (EA, 75 mol%) and *tert*-butyl acrylate (*t*BA, 25 mol%) was conducted to afford the corresponding copolymer, **P4** (Fig. 2A). The number-averaged molar mass (M_n) and degree of molar mass dispersity ($Đ$) were 37,500 g/mol and 2.61, respectively, while the composition was [EA]/[*t*BA] = 71/29. The treatment of the copolymer with trifluoroacetic acid resulted in the selective and quantitative acidolysis of *tert*-butyl ester to yield carboxy (COOH) pendants, as confirmed by ^{1}H NMR (Fig. S12) and IR (Fig. S15) spectra. The rheological properties were dramatically changed by this treatment (Fig. S18), where a clearer rubbery plateau with a higher modulus was observed after acidolysis probably due to the formation of physical cross-links via hydrogen bonds between COOH side groups. The obtained copolymer, **P5**, was cross-linked with 1,6-hexylene bis[α-(bromomethyl)acrylate] (**6**) in tetrahydrofuran (THF) in the presence of excess TEA. The cross-linking reaction was conducted such that the bromine atom contained in **6** became equimolar to the carboxyl pendants of **P5** ([Br]/[COOH] = 1.0). Gelation was observed within 12 s (see Movie-1 in the Supplementary Information), suggesting rapid progress of the cross-linking reaction. The obtained gel was washed with *N*,*N*-dimethylformamide (DMF) three times and with THF three times to remove unreacted TEA, the biproduct of triethylamine hydrobromide, and the sol fraction. Finally, 88% of the total mass of **P5** and **6**, excluding the contribution of liberating HBr, was obtained as the gel fraction. Gelation with different feeding ratios of [Br]/[COOH] for copolymers with various compositions (Table S2, Figs. S9–S17) was also examined (Fig. S19A, Table S3). The gel fraction decreased with an increase in the number of acrylic acid (AA) units, probably due to the formation of a loop structure, that is, intramolecular cross-linking (Fig. S19B). In contrast, the feeding ratio of the cross-linker did not significantly affect gel fraction. Because **P5** cross-linked using an equivalent of **6** ([Br]/[COOH] = 1.0) resulted in the highest gel fraction, the following experiments were conducted using this resin.

As shown in Fig. 2B-a, hot-pressing of the dried cross-linked sample at 140 °C for 2 min did not afford a uniform film, suggesting no processability due to the three-dimensional polymer network structure. The sample was then soaked in THF solution of DABCO and dried again. Remarkably, the hot-pressing of the sample containing 1 wt% DABCO resulted in a film, although it was not transparent and a wrinkled surface was observed (Fig. 2B-b). The increased feeding of DABCO to 10 wt% resulted in a transparent film (Fig. 2B-c). Small-angle X-ray diffraction analysis of this film (Fig. S20) did not exhibit any peaks, suggesting no aggregation of components. Therefore, the film was uniform on the microscopic scale. The realization of simple hot processing to the homogeneous film after the cross-linking formation implies the generation of a covalent adaptable network (CAN), a network cross-linked by DCBs. Feeding DABCO to 54 wt% afforded a sticky film (Fig. 2B-d). In the dynamic mechanical analysis (DMA, Fig. S21) in the temperature sweep mode, the rubbery plateau region was not obvious, and the storage modulus (G') remained close to the loss

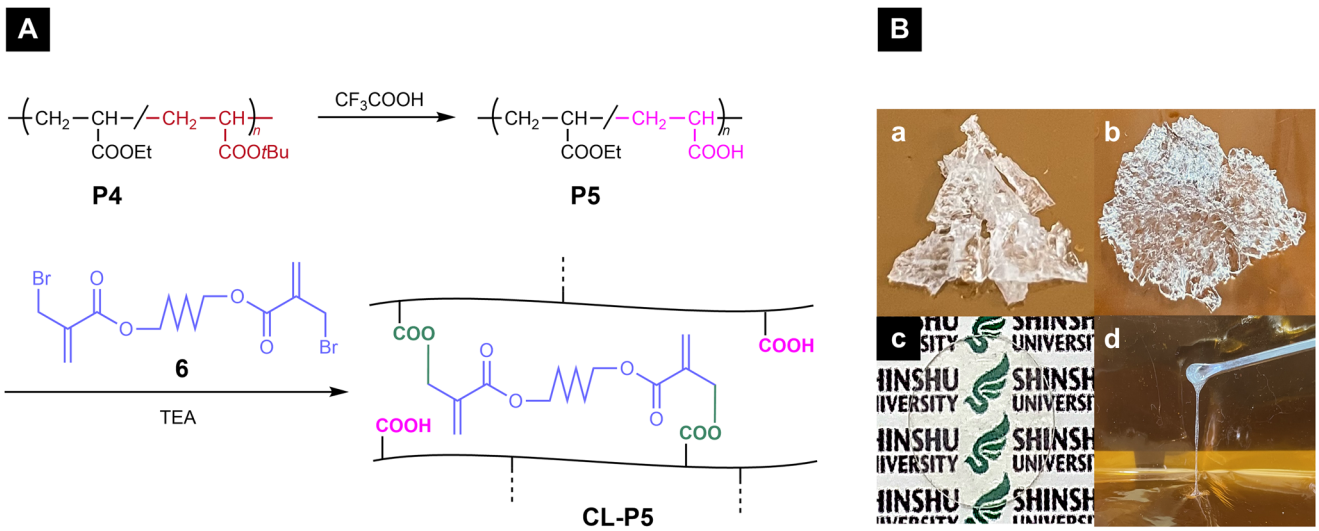

Fig. 2 | Preparation of vitrimer-like acryl elastomers. A Preparation of cross-linked polymers. **B** Photographs of hot-pressed samples without (a) and with 1 wt% (b), 10 wt% (c), and 54 wt% (d) of DABCO.

modulus (G'') above the glass transition, indicating critical gel behavior. In this temperature range, the G' value (<10^5 Pa) was much lower than that of the sample doped with 10 wt% DABCO (>10^6 Pa) (Fig. S22; details of the DMA data are explained in the next section). Therefore, DABCO behaves as a plasticizer and interrupts the formation of a stable cross-linked structure. An obvious flow was observed as the reduction of both G' and G'' occurred at higher temperatures for the sample with 54 wt% DABCO, whereas that with 10 wt% DABCO did not exhibit such behavior. These observations are consistent with the macroscopic appearance. The easier flow can be simply explained by the increase in the catalyst to induce acceleration of bond exchange, where the lowering of the cross-link density due to the plasticity effect should also contribute.

Physical properties and bond exchange characteristics

The suitable amount of DABCO induced processability, where carboxy exchange by a conjugate substitution reaction was the key to the dynamic property of cross-linking. We thus examined the temperature range and time scale for the relaxation induced by the present bond exchange mechanism. The physical properties were investigated for the cross-linked sample of **P5** doped with DABCO (10 wt%) (in the following, this sample is coded **CL-P5**). The DMA curves obtained during the heating process (Fig. 3A) exhibits a clear rubbery plateau, indicating the formation of a cross-linked structure. The DMA curves for both the heating and cooling processes exhibited hysteresis (Fig. S22), which is a common behavior for polymer materials as observed in the precursor linear polymers **P4** and **P5** (Fig. S18). Notably, the plateau modulus (ca. 2.2 MPa) was the same during the cyclic measurements, indicating that the undesired side reaction did not occur and the cross-link density was maintained during the high-temperature treatment. The α relaxation temperature (T_α), originating from the segmental motion, was observed at 20 °C, which is consistent with the T_g (19.0 °C) observed in DSC (Fig. S23). Thermogravimetry–differential thermal analysis (TG-DTA) of **CL-P5** suggested that no thermal degradation occurred over the DMA temperature range (Fig. S24), and the decomposition temperature, defined as the temperature for the 5 wt% loss, was ca. 280 °C. Fig. S25 shows the stress-strain curves of **CL-P5**. The Young's modulus (E_Y) was evaluated as 2.4 MPa and elongation at break was ca. 70%.

The discussion of the plateau modulus, according to the classical rubber elasticity theory for the affine network model (Eq. 1) and phantom network model (Eq. 2)[23], provides information on the network structure, assuming that the contribution from the chain entanglements is small, as in the present design.

$$G_{\text{affine}} = \frac{\rho RT}{M_x} \tag{1}$$

$$G_{\text{phantom}} = \frac{\rho RT}{M_x}\left(1 - \frac{2}{f}\right) \tag{2}$$

In the above equations, M_x indicates the average molecular weight between the cross-links. Because the measured sample after the washing treatment did not contain sol components, the sol effect on the reduction in the modulus was not considered. ρ, R, and T represent polymer density, gas constant, and absolute temperature, respectively. In Eq. 2, the effect of the branch number f at the cross-link point, which is considered as the fluctuation of the cross-links, is expressed in parentheses. Ideally, M_x corresponds to the equivalent molecular weight between the COOH units (M_{COOH}), where M_{COOH} is estimated by M_n/n_{COOH} and n_{COOH} represents the number of COOH units per chain. The plateau modulus is defined here as the minimum tan δ temperature, and the theoretical modulus is estimated to be within the range of 4–8 MPa according to Eqs. 1 and 2. The experimental plateau modulus (2.2 MPa) was much lower than the theoretical value, indicating that there were some network defects that did not contribute to the stress,

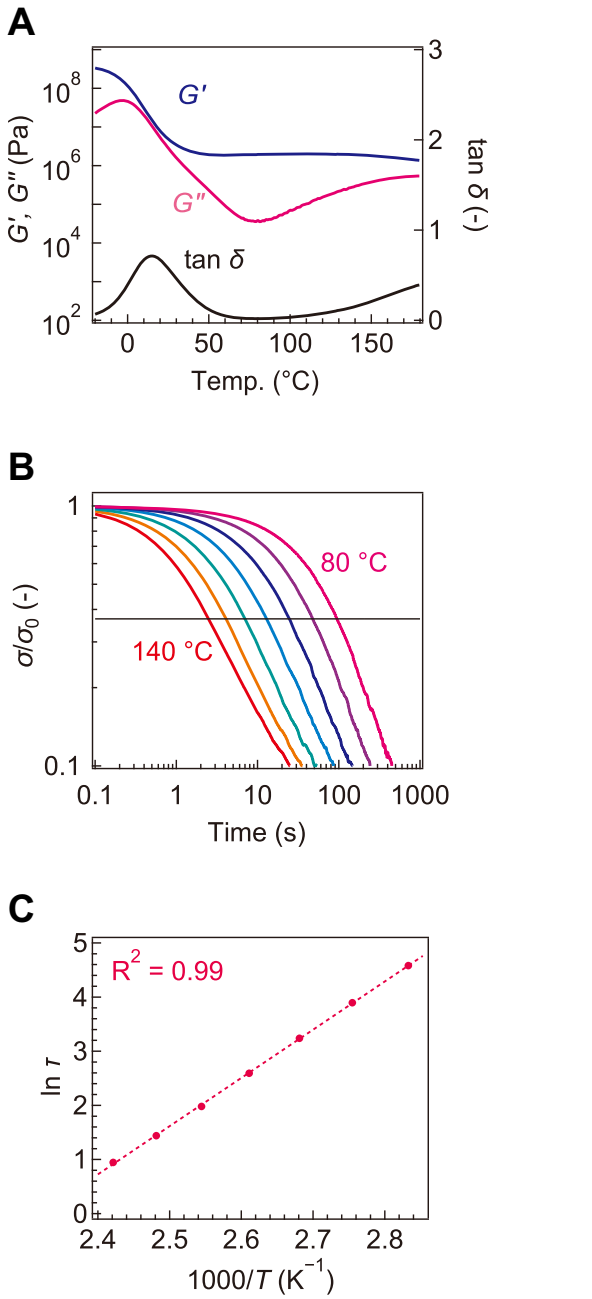

Fig. 3 | Rheological properties of CL-P5. DMA data (**A**), stress-relaxation curves (**B**), and a semi-logarithmic plot of τ against inverse temperatures (**C**) for **CL-P5**. Stress relaxation was performed from 80 to 140 °C at intervals of 10 °C. **B** The stress (σ) is normalized by the initial stress (σ_0).

such as intramolecular cross-links and dangling units[24]. These results are reflected in previous data, showing a relatively low gel fraction of other samples prepared using copolymers with larger AA contents (Fig. S19). This point will be improved in future studies by using other suitable cross-linkers or cross-linking processes.

As another feature in the rubber plateau region of the DMA data, we observed an increase in the loss modulus G'' with an increase in temperature above 100 °C, which accompanied a relaxation in tan δ. These features indicate an increase in strand mobility induced by bond exchange, which is thus analyzed by stress relaxation. Figure 3B shows the normalized stress relaxation data measured in the range of 80–140 °C (>>T_g). The unnormalized relaxation data are shown in Fig. S26A; the initial modulus at $t = 0$ (G_i) monotonically increased with

the temperature at $T \leq 100$ °C (Fig. S26B). According to the DMA data, increases in G'' and tan δ were observed above 100 °C, suggesting that the relaxation originating from the bond exchange was frozen below 100 °C within a measurement time scale of 1 s (i.e., frequency = 1 Hz). In this case, the change in modulus can be treated based on entropic elasticity theory, in which the modulus is proportional to the temperature, which explains the observed monotonic increase in G_i. However, G_i gradually decreased at higher temperatures, indicating a decrease in the temporal cross-link density due to the acceleration of bond exchange. Indeed, the relaxation rate systematically changes with temperature, i.e., the lower the temperature, the slower the relaxation. The relaxation time (τ) was first estimated based on the simple Maxwell model, where τ was determined when the stress decreased to $1/e$ of the initial stress. The temperature dependence of τ followed the Arrhenius function, where the activation energy estimated from the slope was 74 kJ/mol. The Arrhenius dependence of τ is an important feature of bond-exchangeable materials with vitrimer-like properties[25]. As representative values, τ were 95 sec at 80 °C and 2.5 sec at 140 °C (see the values at other temperatures in Table S4). The observed τ will be compared with reported values for various vitrimer systems using poly(meth)acrylate-based components in the later discussion section.

The relaxation properties were analyzed in more detail based on the fitting analysis. The relaxation properties of vitrimers are typically described by stretched exponential functions, so-called Kohlrausch–Williams–Watts (KWW) functions[26,27];

$$\frac{\sigma(t)}{\sigma_0} = \exp\left(-\frac{t}{\tau}\right)^{\beta} \quad (3)$$

In this equation, τ is the specific relaxation time and β is the distribution of τ. The dotted red curve in Fig. 4A represents an example of the fitting curve obtained for data at 100 °C. The fitting was attempted with focusing on the short time region, and the best fit was obtained using $\tau = 18.8$ and $\beta = 0.87$. However, the fitting curve deviated significantly from the experimental curve at the long-time region. Therefore, we tentatively conducted a two-term fitting analysis, assuming that there were two distinct fast and slow relaxation modes.

$$\frac{\sigma(t)}{\sigma_0} = A_{\text{fast}} \exp\left\{-\left(t/\tau_{\text{fast}}\right)^{\beta_{\text{fast}}}\right\} + A_{\text{slow}} \exp\left\{-\left(t/\tau_{\text{slow}}\right)^{\beta_{\text{slow}}}\right\} \quad (4)$$

In the Eq. 4, each parameter with subscript 'fast' and 'slow' corresponds to either fast and slow mode. The coefficients A_{fast} and A_{slow} indicate the contribution fractions of the fast and slow modes, where $A_{\text{fast}} + A_{\text{slow}} = 1$. The dotted black curve in Fig. 4B shows the fitting curve constructed from the fast and slow modes for the data at 100 °C. In this case, the experimental curves were well fitted, and the same fitting was successfully applied to the data at all the other temperatures (Fig. S27 and see the summary of the fitting parameters in Table S5). Notably, A_{fast} was ~0.7 for any temperatures (Table S5), meaning that the major relaxation origin was the fast mode. The values of τ_{fast} and τ_{slow} both followed the Arrhenius dependence with temperatures (Fig. S28), whereas the different activation energy was estimated.

In the following section, we provide an interpretation of the presence of the slow-relaxation mode. A possible reason is related to the effects of chain entanglements. Sumerlin et al. reported the effects of chain entanglements on the relaxation properties of vinylogous urethane vitrimers, revealing that a small increase in the entanglement points reduced the relaxation rate[28]. The molecular weight of the present precursor polymer is much above the expected entanglement molecular weight [≤12,000 g/mol for poly(ethyl acrylate)[29]] and the dispersity of chain length is broad due to the free radical polymerization. Therefore, some portions of the network strand are highly

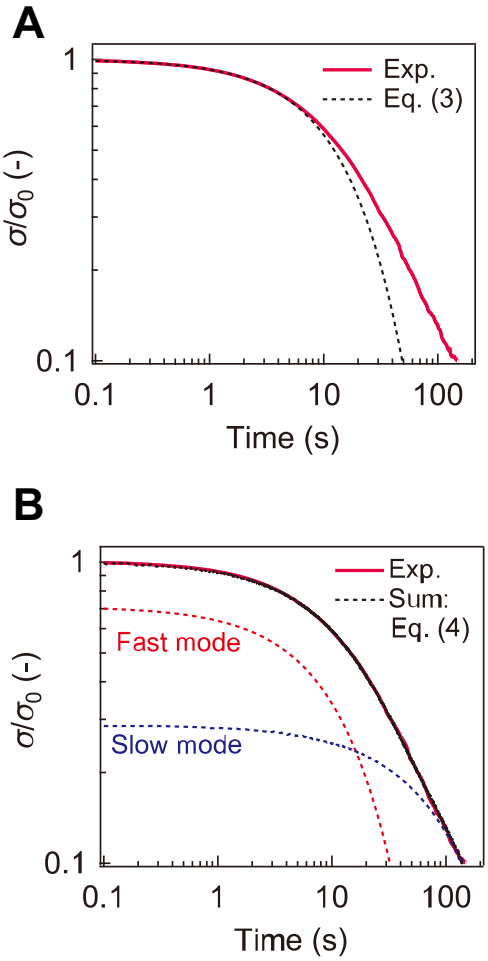

Fig. 4 | Fitting analyses for the stress-relaxation curve of CL-P5 at 100 °C. Fitting analyses based on Eq. (3) (**A**) and Eq. (4) (**B**), respectively.

entangled to induce retardation of the relaxation, which could generate a slow relaxation mode. Another interpretation could be made by focusing on the network structure. In the present network, the cross-linker molecules reacted with the COOH side groups of the precursor polymers not only in an intermolecular manner, but also in an intramolecular manner, according to the discussion of the plateau modulus. In addition, there should be some dangling units generated from the incomplete reaction of the cross-linker molecules. Therefore, there may be some inhomogeneity in the effective cross-link density that provides different relaxation modes. The observation of two distinctive relaxation modes has been actually reported in some studies[30–32], such as for systems containing dual-type bond exchange, block architectures, and filler components.

A model reaction using **1a** and **2b** revealed that the carboxylic acid exchange reaction through a conjugate substitution reaction catalyzed by a tertiary amine progressed even at 25 °C. The solvent effects on the reaction rate were significant; in DMSO, an aprotic polar solvent, 5 min was sufficient for the reaction to reach near-equilibrium. Such high-speed bond exchange was effective for the vitrimer-like elastomers **CL-P5**. The cross-linked polymer was difficult to process into a film, whereas the blend with 10 wt% DABCO afforded a transparent colorless film by simple hot-pressing. Despite its processability, the maintenance of the cross-linked structure was confirmed by the stable rubbery plateau observed in DMA data. In addition, broad tan δ relaxation was observed in the DMA data at high temperature region above 100 °C. This suggests fast stress relaxation comparable to the frequency of DMA (1 Hz). In fact, fast stress relaxation was observed

Table 1 | Properties of selected vitrimers with typical DCBs

Type of DCB	Main monomer	T_g (°C)	τ	Ref.
Disulfide exchange	*n*-Butyl Acrylate (*n*BA)	25	1400 sec at 130 °C	32
Trans-*N*-alkylation of pyridinium	EA	0, −40	800 sec at 150 °C	8
Transesterification	2-Hydroxyethyl methacrylate (HEMA)	100	600 sec at 170 °C	33
Imine exchange	Isobutyl acrylate (*i*BA)	60	500 sec at 120 °C	34
Urethane exchange	*n*BA	60	300 sec at 180 °C	35
Vinylogous-urethane exchange	*n*-Butyl methacrylate	90	30 sec at 150 °C	36
Boronate exchange	Methyl methacrylate (MMA)	100	6.2–18.5 sec at 160 °C	37
Carboxy-exchange by conjugate substitution	EA	19	2.5 sec at 140 °C 95 sec at 80 °C	This work

from 80 °C to 140 °C, τ was 95 s at 80 °C, and 2.5 s at 140 °C. The fast stress-relaxation was attributed to the high-speed carboxy-exchange by the conjugate substitution reaction, which was confirmed in the model reaction at 25 °C. Notably, **CL-P5** was stable in DMSO even at 60 °C (Fig. S29A–C), probably due to the removal of DABCO from the network. In fact, soaking the gel in a 10 wt% DABCO solution in DMSO at 60 °C resulted in a transparent solution (Fig. S29D), suggesting the dissociative DCB by conjugate substitution.

Table 1 summarizes the typical examples of poly(meth)acrylate-based vitrimers[8,33–38] and their relaxation times measured at comparable temperatures. Although the exact comparison must be difficult, due to the difference of T_g and cross-link density, the comparison among the sample with similar low T_g values (i.e., disulfide exchange, trans-*N*-alkylation systems, imine exchange, and urethan exchange, and in Table 1) may be meaningful. The comparison demonstrates that the carboxy-exchange by conjugate substitution reaction can be classified into the significantly fast bond exchange category. Furthermore, it should be emphasized that another advantage of the conjugate substitution reaction is its resistance to moisture, which is in contrast to other high-speed exchange reactions, such as boronate and imine exchange, which are water-sensitive[39–41] and thus require care during the cross-linking reaction and storage. In other words, in addition to efficient bond exchange under mild temperature conditions, the experimental convenience and durability of the material properties are also advantages of the present system.

Fast bond exchange and ease of handling allowed the molding of vitrimer-like elastomers by household products. The **CL-P5** film was cut (Fig. 5A, See Movie-2 in the Supplementary Information), and then a portion of each piece was overlaid on top of each other and heated for 30 s with household iron on a cookie sheet. Even with this simple and mild operation, the films bonded together and did not peel off when a 100 g weight was hung from the film (Fig. 5B, C). Fast bond exchange is also effective for application to an adhesion sheet. A 0.55-mm-thick film of **CL-P5** was cut into a square (1 cm^2) and sandwiched between poly(ethylene terephthalate) (PET) substrates. A 100 g weight was placed on one PET substrate, and the substrates were heated at 60 °C for 1 h. The PET substrates were bonded to each other using the vitrimer-like elastomer film of an adhesive sheet (Fig. 5D). The bonded PET substrates were subjected to a load in increments of 1 kg and the interface was peeled off at 3 kg (Fig. 5E). Similar experiments were conducted with PMMA and aluminum substrates, both of which retained their adhesion up to 1 kg of load. The polystyrene substrate withstood a load of 500 g and was delaminated to 1 kg. Overall, heating at 60 °C for 1 h resulted in adhesive strength, which was attributed to the sufficiently fast bond exchange of the vitrimer-like elastomers, even at this temperature.

In conclusion, we propose a new molecular design of bond-exchangeable cross-link materials based on carboxy-exchange by conjugate substitution reaction. First, the model reactions using small molecules suggested that the carboxy-exchange works as a DCB operated at ambient temperature. We further demonstrated that

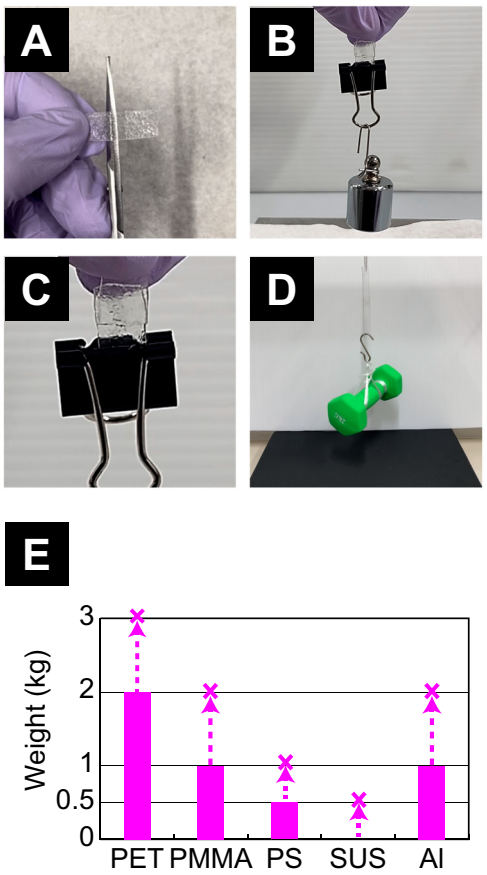

Fig. 5 | Adhesion tests of CL-P5. Cut film of **CL-P5** (**A**) and self-adhered films with a weight of 100 g (**B**, **C**). The red arrows indicate the self-adhered areas. The PET substrates were bonded using a sheet of **CL-P5** with a weight of 2 kg (**D**). Strengths of the adhesion sheets on each substrate (**E**). The cross marks indicate weights at peeling off.

carboxy-exchange is effective in vitrimer-like elastomer applications. The cross-linked polymers, prepared using copolymers of AA with **6** and doped with DABCO, exhibited significantly faster stress relaxation and thus enabled easy and quick operation of the useful functions compared with the reported systems. All the experiments were performed in an ambient environment, and the cross-linking agent was commercially available. This convenience is also an attraction for the present design concept using conjugate substitution reactions. Dynamic cross-linking via conjugate substitution reactions can be applied to a wide variety of polymers bearing carboxy pendants, which is important for the preparation of practical vitrimer-like elastomers. Thus, we believe that our approach has potential applications in material science and engineering.

Methods

Materials

Chloroform-d_1 ($CDCl_3$, 99.8 atom % D with 0.03 vol% tetramethylsilane) and dimethyl sulfoxide-d_6 (DMSO-d_6, 99.9 atom % D), were purchased from Kanto Chemical Co., Inc. 1,4-Diazabicyclo[2.2.2.]octane (DABCO), 1,5,7-triazabicyclo[4.4.0]dec-5-ene (TBD), trifluoroacetic acid (TFA), ethyl acrylate (EA), *tert*-butyl acrylate (*t*BA) were purchased from Tokyo Chemical Industry Co., Ltd. Triethylamine (TEA), 2,2′-azobisisobutyronitrile (AIBN), 1,4-dioxane, dichloromethane and tetrahydrofuran (THF) were purchased from Fujifilm Wako Pure Chemical Industry Co. *N*,*N*-Dimethylformamide (DMF) was purchased from Kishida Chemical Co., Ltd. Diethyl ether was purchased from Yoneyama Yakuhin Kogyo Co., Ltd. 1,6-hexylene bis[α-(bromomethyl)acrylate] (**6**) was purchased from Chemicrea Inc. Methyl 2-(acetoxymethyl)acrylate (**1a**) was prepared according to the literature[42].

^{1}H NMR spectrometry

^{1}H spectra were recorded in $CDCl_3$ or DMSO-d_6 on an AVANCE NEO (Bruker) spectrometers. Chemical shifts in ^{1}H NMR spectra were referred to the signal of tetramethylsilane (TMS) and solvent ($CHCl_3$ or DMSO), respectively.

IR spectrometry

IR spectra were recorded on a Cary 630 FTIR spectrometer equipped with a diamond-attenuated total reflection (ATR) accessory.

Size-exclusion chromatography

Molecular weight and its distributions were determined at 40 °C by size-exclusion chromatography (SEC) on an EXTREMA chromatograph (JASCO) equipped with two SEC columns [PL-gel, Mixed C (300 mm × 7.5 mm), Polymer Laboratories], using 0.01 M LiBr in DMF as an eluent (flow rate = 0.8 mL min^{-1}), and calibrated against standard poly(methyl methacrylate) (PMMA) samples (TSK-gel oligomer kit, Tosoh, M_n: 6.03×10^5, 2.52×10^5, 1.42×10^5, 2.91×10^4, 8.59×10^3, 4.25×10^3, 1.46×10^3, 8.30×10^2) and detected with UV (UV-4070, JASCO) and RI (RI-4030, JASCO) detectors.

Thermal analysis

Thermogravimetric/differential thermal analysis (TG/DTA) was carried out from room temperature to 500 °C at a heating rate of 10 °C min^{-1} with Rigaku Thermo plus II TG8120 under an N_2 atmosphere. Differential scanning calorimetry (DSC) was performed at a heating rate of 20 °C min^{-1} with Rigaku Thermo plus II TG8230 under an N_2 atmosphere.

Dynamic mechanical analysis (DMA) and stress-relaxation test

The specimen with a thickness of 0.5 mm was prepared by hot pressing at 140 °C for 2 min. A disc-shaped sample with an 8 mm diameter and ~0.5 mm thickness was measured. DMA was assessed using a shear-type rheometer, MCR102e (Anton Paar), and a disposable 8 mm plate. The frequency was fixed at 1 Hz, and a constant strain of 0.1% was applied. A cyclic cooling and heating measurement was performed with a temperature change rate of 2 °C/min.

The stress–relaxation tests for the cross-linked samples were conducted at various high temperatures with the same setup. The strain was fixed to be 3%, which was within the linear regime. The samples for the measurements were initially dried by a vacuum for 12 h, and all the above rheology measurements were conducted under N_2 gas to minimize effects of moisture in the air.

Tensile test

Tensile test was performed on an AGS-500NX (Shimadzu) using the dumbbell-shaped specimen with a thickness of 4 mm. The measurement was performed at 25 °C at the 10 mm/min of extension speed.

Synthesis

Carboxylic acid exchange reaction between methyl α-(acetoxymethyl) acrylate (**1a**) and benzoic acid (**2b**): A typical example using TEA in $CDCl_3$:**1a** (0.158 g, 1.00 mmol) and **2b** (0.122 g, 1.00 mmol) were dissolved in $CDCl_3$ (0.40 mL), and decamethylcyclopentanesiloxane (ca. 10 mg) was added as an internal standard. The NMR spectrum was measured as an initial sample (Fig. S1, before). TEA (10 mg, 0.10 mmol) was added to the sample to start the reaction. The ^{1}H NMR spectra were recorded at the determined periods. For the measurement in DMSO-d_6, DMF was used as an internal standard.

Copolymerization of EA and tBA (Synthesis of P4, P7, and P9). A typical example for **P4**. A solution of EA (6.00 g, 60.0 mmol), *t*BA (2.56 mmol, 20.0 mmol), and AIBN (49 mg, 0.30 mmol) in 1,4-dioxane (40 mL) was degassed by N_2 gas bubbling for 20 min, and the copolymerization was conducted at 70 °C for 24 h. The reaction mixture was cooled and poured into a cosolvent of water–methanol (300 mL /600 mL). The supernatant was removed by decantation, and the collected precipitate was dried *in vacuo* to afford **P4**. Yield: 7.73 g, 90.3%; M_n = 37500 g/mol, $Đ$ = 2.62; [EA]/[*t*BA] = 71/29. The composition was determined from ^{1}H NMR spectrum (Fig. S8) as the intensity ratio of *O*-CH_2 signal of EA units at 4.2 ppm and *tert*-butyl signal of *t*BA units at 1.1 ppm.

The feeding ratio of reagents and results for other entries were summarized in Table S2.

Synthesis of the copolymer of EA and AA (P5, P8, and P10). A typical example for **P5**. The copolymer obtained above (**P4**, 7.73 g, 20.7 mmol for *t*BuA unit) was dissolved in dichloromethane (40 mL), and TFA (15 mL) was added to the solution. The reaction mixture was stirred for 24 h and concentrated. The residue was diluted with THF (10 mL) and poured into diethyl ether (1000 mL). The precipitate was collected by centrifugation and dried *in vacuo* to afford **P5** as a sticky solid. Yield: 4.04 g, 61.5%; M_n, estimated as a theoretical value from **P4**, was 31800 g/mol.

Cross-linking reaction. A typical procedure for **P5**. TEA (66 mg, 65 mmol) was added to a solution of **P5** (0.200 g, 0.624 mmol for AA units, 1.53 mmol for EA units) and **6** (0.125 g, 0.326 mmol) in THF (0.30 mL). The gel was formed within 12 sec with white precipitation. After 12 h, the gel was soaked in DMF (20 mL) for 12 h, and the supernatant was removed by decantation. This procedure was repeated once, and similar procedure using THF (20 mL) instead of DMF was repeated twice. Finally, the gel was dried *in vacuo* to afford a cross-linked polymer, **P5-30** (2.6 g, 88%). The feeding ratio of reagents and results for other entries were summarized in Table S3.

DABCO addition to the cross-linked sample. A typical procedure for **P5-30**.**P5-30** (50.2 mg) was soaked in a solution of DABCO (5.8 mg, 10 wt% for total mass of composite) in THF (0.1 mL) at 25 °C for 12 h. The solution was completely absorbed to form a swollen gel. This gel was dried in vacuo (<10 mmHg) at 25 °C for 12 h. The dried sample was hot-pressed at 140 °C for 2 min. Similar experiments were performed using 0.7 mg (1 wt%) and 58 mg (54 wt%) of DABCO.

Data availability

The authors declare that the data supporting the findings of this study are available within the paper and its Supplementary Information files. Should any raw data files be needed in another format they are available from the corresponding author upon request.

References

1. Montarnal, D., Capelot, M., Tournilhac, F. & Leibler, L. Silica-like malleable materials from permanent organic networks. *Science* **334**, 965–968 (2011).

2. Zheng, N., Xu, Y., Zhao, Q. & Xie, T. Dynamic covalent polymer networks: a molecular platform for designing functions beyond chemical recycling and self-healing. *Chem. Rev.* **121**, 1716–1745 (2021).
3. Shi, Q., Jin, C., Chen, Z., An, L. & Wang, T. On the welding of vitrimers: chemistry, mechanics and applications. *Adv. Funct. Mater.* **33**, 2300288 (2023).
4. Scheutz, G. M., Lessard, J. J., Sims, M. B. & Sumerlin, B. S. Adaptable crosslinks in polymeric materials: resolving the intersection of thermoplastics and thermosets. *J. Am. Chem. Soc.* **141**, 16181–16196 (2019).
5. Winne, J. M., Leibler, L. & Du Prez, F. E. Dynamic covalent chemistry in polymer networks: a mechanistic perspective. *Polym. Chem.* **10**, 6091–6108 (2019).
6. Guerre, M., Taplan, C., Winne, J. M. & Du Prez, F. E. Vitrimers: directing chemical reactivity to control material properties. *Chem. Sci.* **11**, 4855–4870 (2020).
7. Denissen, W., Winne, J. M. & Du Prez, F. E. Vitrimers: permanent organic networks with glass-like fluidity. *Chem. Sci.* **7**, 30–38 (2016).
8. Oba, Y., Kimura, T., Hayashi, M. & Yamamoto, K. Correlation between self-assembled nanostructures and bond exchange properties for polyacrylate-based vitrimer-like materials with a trans-N-alkylation bond exchange mechanism. *Macromolecules* **55**, 1771–1782 (2022).
9. Obadia, M. M., Jourdain, A., Cassagnau, P., Montarnal, D. & Drockenmuller, E. Tuning the viscosity profile of ionic vitrimers incorporating 1,2,3-triazolium cross-links. *Adv. Funct. Mater.* **27**, 1703258 (2017).
10. Van Herck, N. & Du Prez, F. E. Fast healing of polyurethane thermosets using reversible triazolinedione chemistry and shape-memory. *Macromolecules* **51**, 3405–3414 (2018).
11. Liu, T., Zhao, B. & Zhang, J. Recent development of repairable, malleable and recyclable thermosetting polymers through dynamic transesterification. *Polymer* **194**, 122392 (2020).
12. Jourdain, A. et al. Rheological properties of covalent adaptable networks with 1,2,3-triazolium cross-links: the missing link between vitrimers and dissociative networks. *Macromolecules* **53**, 1884–1900 (2020).
13. Hao, C. et al. Triethanolamine-mediated covalent adaptable epoxy network: excellent mechanical properties, fast repairing, and easy recycling. *Macromolecules* **53**, 3110–3118 (2020).
14. Spitzbarth, B. & Eelkema, R. Chemical reaction networks based on conjugate additions on β′-substituted Michael acceptors. *Chem. Commun.* **59**, 11174–11187 (2023).
15. Zhuang, J. M. et al. A programmable chemical switch based on triggerable Michael acceptors. *Chem. Sci.* **11**, 2103–2111 (2020).
16. Klemm, B., Lewis, R. W., Piergentili, I. & Eelkema, R. Temporally programmed polymer - solvent interactions using a chemical reaction network. *Nat. Commun.* **13**, 6242 (2022).
17. Kohsaka, Y., Miyazaki, T. & Hagiwara, K. Conjugate substitution and addition of alpha-substituted acrylate: a highly efficient, facile, convenient, and versatile approach to fabricate degradable polymers by dynamic covalent chemistry. *Polym. Chem.* **9**, 1610–1617 (2018).
18. Xu, Y. C., Ren, W. M., Zhou, H., Gu, G. G. & Lu, X. B. Functionalized polyesters with tunable degradability prepared by controlled ring-opening (co)polymerization of lactones. *Macromolecules* **50**, 3131–3142 (2017).
19. Noda, T., Kitagawa, T. & Kohsaka, Y. Degradation of poly(conjugated ester)s using a conjugate substitution reaction with various amines and amino acids in aqueous media. *Polym. J.* **56**, 1–9 (2023).
20. Noda, T., Tanaka, A., Akae, Y. & Kohsaka, Y. Unsaturated polyurethanes degradable by conjugate substitution reactions with amines and carboxylate anions. *RSC Adv* **13**, 20336–20341 (2023).
21. Kohsaka, Y. Conjugate substitution reaction of alpha-(substituted methyl)acrylates in polymer chemistry. *Polym. J.* **52**, 1175–1183 (2020).
22. Kohsaka, Y., Akae, Y., Kawatani, R. & Kazama, A. Polymer chemistry of alpha-substituted acrylates designed for functional-group synergy. *J. Macromol. Sci. Part A-Pure App. Chem.* **59**, 83–97 (2022).
23. Rubinstein, M. *Polymer physics*. (Oxford University Press, 2003).
24. Mark, J. E. & Erman, B. *Rubberlike elasticity: a molecular primer*. (Cambridge University Press, 2007).
25. Wu, S. & Chen, Q. Advances and new opportunities in the rheology of physically and chemically reversible polymers. *Macromolecules* **55**, 697–714 (2022).
26. Hayashi, M., Yano, R. & Takasu, A. Synthesis of amorphous low Tg polyesters with multiple COOH side groups and their utilization for elastomeric vitrimers based on post-polymerization cross-linking. *Polym. Chem.* **10**, 2047–2056 (2019).
27. Kimura, T. & Hayashi, M. One-shot transformation of ordinary polyesters into vitrimers: decomposition-triggered cross-linking and assistance of dynamic covalent bonds. *J. Mater. Chem. A Mater. Energy Sustain.* **10**, 17406–17414 (2022).
28. Lessard, J. J., Stewart, K. A. & Sumerlin, B. S. Controlling dynamics of associative networks through primary chain length. *Macromolecules* **55**, 10052–10061 (2022).
29. Andreozzi, L., Castelvetro, V., Faetti, M., Giordano, M. & Zulli, F. Rheological and thermal properties of narrow distribution poly(ethyl acrylate)s. *Macromolecules* **39**, 1880–1889 (2006).
30. Van Lijsebetten, F., De Bruycker, K., Van Ruymbeke, E., Winne, J. M. & Du Prez, F. E. Characterising different molecular landscapes in dynamic covalent networks. *Chem. Sci.* **13**, 12865–12875 (2022).
31. Hayashi, M. & Chen, L. Functionalization of triblock copolymer elastomers by cross-linking the end blocks via trans-N-alkylation-based exchangeable bonds. *Polym. Chem.* **11**, 1713–1719 (2020).
32. Kimura, T. & Hayashi, M. Exploring the effects of bound rubber phase on the physical properties of nano-silica composites with a vitrimer-like bond exchangeable matrix. *Polym. J.* **54**, 1307–1319 (2022).
33. Yamawake, K. & Hayashi, M. The role of tertiary amines as internal catalysts for disulfide exchange in covalent adaptable networks. *Polym. Chem.* **14**, 680–686 (2023).
34. Debnath, S., Kaushal, S. & Ojha, U. Catalyst-free partially bio-based polyester vitrimers. *ACS Appl. Polym. Mater.* **2**, 1006–1013 (2020).
35. Miao, J.-T. et al. Dynamic imine bond-based shape memory polymers with permanent shape reconfigurability for 4D printing. *ACS Appl. Mater. Interfaces* **11**, 40642–40651 (2019).
36. Niu, X. et al. Self-healing, thermadapt triple-shape memory ionomer vitrimer for shape memory triboelectric nanogenerator. *ACS Appl. Mater. Interfaces* **14**, 50101–50111 (2022).
37. Lessard, J. J. et al. Block copolymer vitrimers. *J. Am. Chem. Soc.* **142**, 283–289 (2020).
38. Wang, Z., Gu, Y., Ma, M. & Chen, M. Strong, reconfigurable, and recyclable thermosets cross-linked by polymer–polymer dynamic interaction based on commodity thermoplastics. *Macromolecules* **53**, 956–964 (2020).
39. Luo, J. et al. Elastic vitrimers: Beyond thermoplastic and thermoset elastomers. *Matter* **5**, 1391–1422 (2022).
40. Cromwell, O. R., Chung, J. & Guan, Z. Malleable and self-healing covalent polymer networks through tunable dynamic boronic ester bonds. *J. Am. Chem. Soc.* **137**, 6492–6495 (2015).
41. Taynton, P. et al. Re-healable polyimine thermosets: polymer composition and moisture sensitivity. *Polym. Chem.* **7**, 7052–7056 (2016).
42. Katsina, T. et al. Sequential palladium-catalyzed allylic alkylation/retro-dieckmann fragmentation strategy for the synthesis of α-substituted acrylonitriles. *Org. Lett.* **21**, 9348–9352 (2019).

Acknowledgements
This research was financially supported by JST PRESTO Grant Numbers JPMJPR22N4 (for Y.K.) and JPMJPR23N7 (for M.H.). The authors thank Dr. Yusuke Okada (Shinshu University) for the tensile testing.

Author contributions
N.N.: validation, formal analysis, investigation, visualization. R.K.: validation, methodology. S.T.: validation, formal analysis, investigation. M.M.: validation, formal analysis, investigation. M.H.: methodology, formal analysis, investigation, data curation, writing–review & editing, supervision, funding acquisition. Y.K.: conceptualization, methodology, data curation, writing–original draft, visualization, supervision, project administration, funding acquisition.

Competing interests
Y.K. has a patent (Japanese Patent No. 7441526) on the cross-linking reaction and the cross-linked polymers issued to Shinshu University. The remaining authors declare no competing interests.

Additional information
Supplementary information The online version contains supplementary material available at https://doi.org/10.1038/s41467-024-53043-5.

Correspondence and requests for materials should be addressed to Mikihiro Hayashi or Yasuhiro Kohsaka.

Peer review information *Nature Communications* thanks Pere Verdugo Fernández and the other, anonymous, reviewer(s) for their contribution to the peer review of this work. A peer review file is available.